IEEE Access
Multidisciplinary | Rapid Review | Open Access Journal

Received August 20, 2020, accepted September 2, 2020, date of publication September 9, 2020,
date of current version September 24, 2020.

Digital Object Identifier 10.1109/ACCESS.2020.3022846

An Improved Lightning Attachment Procedure Optimizer for Optimal Reactive Power Dispatch With Uncertainty in Renewable Energy Resources

MOHAMED EBEED[1], ABDELFATAH ALI[2], MOHAMED I. MOSAAD[3], AND SALAH KAMEL[4]
[1]Department of Electrical Engineering, Faculty of Engineering, Sohag University, Sohag 82524, Egypt
[2]Department of Electrical Engineering, Faculty of Engineering, South Valley University, Qena 83523, Egypt
[3]Department of Electrical and Electronic Engineering, Yanbu Industrial College, Yanbu 46452, Saudi Arabia
[4]Department of Electrical Engineering, Faculty of Engineering, Aswan University, Aswan 81542, Egypt

Corresponding authors: Mohamed I. Mosaad (habibm@rcyci.edu.sa) and Salah Kamel (skamel@aswu.edu.eg)

This work was supported in part by the NSFC, China-ASRT, Egypt, Joint Research Fund, under Grant 51861145406.

ABSTRACT Integrating renewable energy resources (RERs) has become the head of concern of the modern power system to diminish the dependence of using conventional energy resources. However, intermittent, weather dependent, and stochastic natural are the main features of RESs which lead to increasing the uncertainty of the power system. This paper addresses the optimal reactive power dispatch (ORPD) problem using an improved version of the lightning attachment procedure optimization (LAPO), considering the uncertainties of the wind and solar RERs as well as load demand. The improved lightning attachment procedure optimization (ILAPO) is proposed to boost the searching capability and avoid stagnation of the traditional LAPO. ILAPO is based on two improvements: i) Levy flight to enhance the exploration process, ii) Spiral movement of the particles to improve the exploitation process of the LAPO. The scenario-based method is used to generate a set of scenarios captured from the uncertainties of solar irradiance and wind speed as well as load demand. The proposed ILAPO algorithm is employed to, optimally, dispatch the reactive power in the presence of RERs. The power losses and the total voltage deviations are used as objective functions to be minimized. The proposed algorithm is validated using IEEE 30-bus system under deterministic and probabilistic conditions. The obtained results verified the efficacy of the proposed ILAPO for ORPD solution compared with the traditional LAPO and other reported optimization algorithms.

INDEX TERMS Optimal reactive power dispatch, renewable energy, lightning attachment procedure optimization, power losses, uncertainty.

LIST OF ABBREVIATIONS

ALO	Ant Lion Optimizer
BBO	Biogeography-Based Optimization
CSA	Cuckoo Search Algorithm
CLPSO	Comprehensive Learning PSO
FA	Firefly Algorithm
GSA	Gravitational Search Algorithm
GSA-CSS	Gravitational Search Algorithm Conditional Selection Strategies
HSA	Harmony Search Algorithm
HPSO–TS	Hybrid PSO with the Tabu Search
HSSSA	Hybrid Salp Swarm Algorithm and Simulated Annealing
IPG-PSO	Improved Pseudo-Gradient PSO
ISSO	Improved Social Spider Optimization
JA	Jaya Algorithm
IDE	Improved Differential Evolution
IGSALAPO-CSS	Improved GSA-CSS
IALO	Improved Antlion Optimization
LAPO	Lightning Attachment Procedure Optimization
ILAPO	Improved Lightning Attachment Procedure Optimization
MSSA	Modified Salp Swarm Algorithm
ORPD	Optimal Reactive Power Dispatch
PSO	Particle Swarm Optimization
PSO-TVAC	PSO with Time-Varying Acceleration Coefficients

The associate editor coordinating the review of this manuscript and approving it for publication was Canbing Li.

PSO-TVIW	PSO with Time-Varying Inertia Weight
PG-PSO	PSO with Pseudo Gradient Search
PSO-CF	PSO With Constriction Factor
SPSO-TVAC	PSO with Time-Varying Acceleration Coefficients
PSO-TVAC	PSO with Time-Varying Acceleration Coefficients
TLBO	Teaching Learning Based Optimization
SGA	Specialize Ed Genetic Algorithm
RERs	Renewable Energy Resources
SSO	Social Spider Optimization
SSA	Salp Swarm Algorithm
STGA	Standard Genetic Algorithm
QOTLBO	Quasi-Oppositional Teaching Learning Based Optimization
TS	Tabu Search
WOA	Whale Optimization Algorithm

I. INTRODUCTION

The problem of optimal reactive power dispatch (ORPD) is an important task to be solved for improving the performance, security, and reliability of electrical systems. ORPD is based on assigning the best operating point, which includes the voltages of generation units, transformer taps, and the reactive power of the compensators for diminishing the power losses, enhancing the voltage profile, and the system stability while satisfying the system constraints [1].

ORPD problem is a non-convex, complex, and nonlinear optimization problem. Thus, many efforts have been introduced for solving the ORPD by applying numerous optimization techniques including the Backtracking Search Optimizer (BSO) [2], Particle Swarm Optimization (PSO) [3], Ant Lion Optimizer (ALO) [4], Improved Ant Lion Optimization algorithm (IALO) [5], Whale Optimization Algorithm (WOA) [6], Improved Social Spider Optimization Algorithm (ISSO) [7], Differential Evolution (DE) [8], Moth Swarm Algorithm (MSA) [9], Evolutionary Algorithm (EA) [10], Modified Differential Evolution (MDE) [11], Jaya Algorithm (JA) [12], Modified Sine Cosine Algorithm (MSCA) [13], Lightning Attachment Procedure Optimization (LAPO) [14], Gravitational Search Algorithm (GSA) [15], Biogeography-Based Optimization (BBO) [16], Teaching Learning Based Optimization (TLBO) [17], Harmony Search Algorithm (HAS) [17], Grey Wolf Optimizer (GWO) [18], Comprehensive Learning Particle Swarm Optimization (CLPSO) [19], Chemical Reaction Optimization (CRO) [20], Improved Gravitational Search Algorithm (IGSA) [21], Improved Pseudo-Gradient Search Particle Swarm Optimization (IPG-PSO) [22], Firefly Algorithm (FA) [23], Fractional Particle Swarm Optimization Gravitational Search Algorithm [24], hybrid GWO-PSO optimization [25], Oppositional Salp Swarm Algorithm (OSSA) [26], diversity-enhanced particle swarm optimization (DEPSO) [27].

Several problems are related to RERs, including the stochastics natural and the continuous fluctuations which lead to the uncertainties in power systems. Thereby, it is an important issue to consider the uncertainties of RERs for efficient planning. Several papers were presented to solve the ORPD with taken into consideration the uncertainty in the power system. In [28], the adaptive differential evolution has been utilized to address the ORPD, and the uncertainties of RERs and loads were considered using a scenario-based strategy. In [29], have the Quantum-behaved particle swarm optimization differential mutation (QPSODM) has been employed for solving the ORPD under RERs and load uncertainties on the practical Adrar's power system and IEEE 14-bus. The MSA has been used for solving the ORPD considering the stochastic natural RERs and load [9]. In [30], have solved the ORPD, considering the uncertainties of the wind and load powers. In [31], the two-point estimation method has been applied for uncertainty modelling of the load for solving ORPD.

LAPO is a recent algorithm presented by Nematollahi *et al.* [32], [33]. LAPO mimics the lightning procedure phenomenal, it starts from initial spots, which mimic the initial solutions, and the strike point mimics optimal solution and movement of the uploaders, and downloaders simulate the updating process of the optimization algorithm. LAPO has been implemented to solve numerous optimization problems. the authors in [34] have implemented the LAPO technique to find the best position and sizing of the unified power flow controller in the transmission system. Y. Heba *et al.* used the LAPO for solving the OPF problem [35]. In [36], the LAPO technique has been used to assign the optimal ratings and placement of the DGs in the distribution grid. W. Lui *et al.* have applied the LAPO for optimization the image segmentation [37]. It should be pointed out that LAPO may be tripped to local optima in some cases. Thus, an improved LAPO is proposed to solve the stagnation of LAPO.

The main paper contributions can be itemized as:

1- Proposing a modified version of the traditional LAPO using levy flight and spiral movement to improve the searching abilities.
2- Applying the proposed algorithm to address the ORPD problem under inclusion RERs.
3- The ORPD is solved under the uncertainties of load demand and the RERs including the wind and solar PV sources.
4- The scenario-based method is utilized to produce a set of scenarios to combine scenarios of the load, solar irradiance, and wind speed.
5- The proposed algorithm is applied and validated using IEEE 30-bus system and compared with other techniques.

The arrangement the paper is adjusted as follows: Section 2 describes the problem formulation. Section 3 explains the uncertainty modeling in the power system. An overview of LAPO and ILAPO is depicted in Section 4. The captured results are shown in Section 5. Finally, the paper conclusions are listed depicted in Section 6.

II. PROBLEM FORMULATION

The main task of the ORPD is assigning the optimal operating point for power losses and voltage deviation minimization as well as the stability enhancement with satisfying the system constraints. The ORPD problem is described as follows:

$$Min\ F(x,u) \tag{1}$$

$$\text{Subjected to } g_k(x,u)=0 \quad k=1,2,\ldots,m \tag{2}$$

$$h_n(x,u)\le 0 \quad n=1,2,\ldots,p \tag{3}$$

where, g_k and h_n denotes the equality and inequality constraints. u and x are two vectors of the control and the dependent variables as depicted in equations (4) and (5)

$$u=[V_G,Q_C,T_p] \tag{4}$$

$$x=[P_1,V_L,Q_G,S_T] \tag{5}$$

where, V_G, Q_C, and T_p are the generator voltage, reactive power of the capacitor, and the transformer tap, respectively. P_1, V_L, Q_G, and S_T are the slack bus power, voltage of the load bus, and apparent power flow in the transmission line, respectively.

A. OBJECTIVE FUNCTION

1) POWER LOSSES

$$F_{obj1}=P_{Loss}=\sum_{i=1}^{N_L}G_{ij}(V_i^2+V_j^2-2V_iV_jcos\delta_{ij}) \tag{6}$$

where P_{Loss} represents the power losses; G_{ij} is the conductance of the transmission line between buses i and j; N_L is the number of the transmission lines.

2) VOLTAGE DEVIATIONS

$$F_{obj2}=TVD=\sum_{i=1}^{N_Q}|(V_i-1)| \tag{7}$$

where TVD is the summation of the voltage deviations; N_Q is the number of PQ buses.

B. CONSTRAINTS

1) INEQUALITY CONSTRAINTS

$$P_1^{\min}\le P_1\le P_1^{\max} \quad k=1,2,\ldots,N_G \tag{8}$$

$$Q_{Gk}^{min}\le Q_{Gk}\le Q_{Gk}^{max} \quad k=1,2,\ldots,N_G \tag{9}$$

$$V_{Gk}^{min}\le V_{Gk}\le V_{Gk}^{max} \quad n=1,2,\ldots,N_G \tag{10}$$

$$T_p^{min}\le T_p\le T_p^{max} \quad n=1,2,\ldots,N_T \tag{11}$$

$$Q_{Cn}^{min}\le Q_{Cn}\le Q_{Cn}^{max} \quad n=1,2,\ldots,N_C \tag{12}$$

$$S_{Ln}\le S_{Ln}^{min} \quad n=1,2,\ldots,N_L \tag{13}$$

$$V_n^{min}\le V_n\le V_n^{max} \quad n=1,2,\ldots,N_Q \tag{14}$$

where min and max are superscripts for the minimum and maximum limit of the dependent and control variables; N_G is the number of generators; N_T is the number of taps, N_L the number of transmission lines.

2) QUALITY CONSTRAINTS

$$P_{Gi}-P_{Li}=V_i\sum_{j=1}^{Nb}V_j[G_{ij}cos(\delta_i-\delta_j)+B_{ij}sin(\delta_i-\delta_j)] \tag{15}$$

$$Q_{Gi}-Q_{Li}=V_i\sum_{j=1}^{NB}V_j[G_{ij}cos(\delta_i-\delta_j)-B_{ij}sin(\delta_i-\delta_j)] \tag{16}$$

where B_{ij} is the substance of the TL between buses i and j. δ_i and δ_j are the voltage angles of buses i and j, respectively. To avoid any violation of the system constraints, they should be considered in objective function weighted square variables as follows:

$$\begin{aligned}F=F_i&+k_1\left(P_{G1}-P_{G1}^{lim}\right)^2\\&+k_2\sum_{i=1}^{N_G}\left(Q_{Gi}-Q_{Gi}^{lim}\right)^2\\&+k_3\sum_{i=1}^{N_Q}\left(V_{Li}-V_{Li}^{lim}\right)^2\\&+k_4\sum_{i=1}^{N_l}\left(S_{Li}-S_{Li}^{lim}\right)^2\end{aligned} \tag{17}$$

where k_1, k_2, k_3, and k_4 are the penalty factors. lim is a superscript denotes the allowable maximum or the minimum limit.

III. UNCERTAINTY MODELING

Three uncertainty parameters are considered in this study, including load demand and wind and PV sources, which depend upon the wind speed and solar irradiance. The probability density functions (pdfs) are utilized for modeling these uncertainties where the continuous is divided into subsections to obtain a set of scenarios.

A. THE UNCERTAINTY OF LOAD DEMAND

The normal PDF is utilized to model the uncertainty of load demand as follows [30]:

$$PDF_L(P_L)=\frac{1}{\sigma_L\sqrt{2\pi}}exp\left[-\frac{(P_L-\mu_L)2}{2\sigma_L^2}\right] \tag{18}$$

where σ_L and μ_L denote the standard deviation and mean values, respectively. The selected values of the σ_L and μ_L are 70 and 10, respectively [28]. The portability of load demands and the followed expected load scenarios are obtained as [38]:

$$\pi_{L,i}=\int_{P_{L,i}^{min}}^{P_{L,i}^{max}}PDF_L(P_L)dP_L \tag{19}$$

$$P_{L,i}=\frac{1}{\pi_{L,i}}\int_{P_{L,i}^{min}}^{P_{L,i}^{max}}P_L\times PDF_L(P_L)dP_L \tag{20}$$

where $P_{L,i}^{max}$ and $P_{L,i}^{min}$ represent the maximum and the minimum limits of the selected interval i. Three scenarios of load demand are generated in this paper. By applying the

previous equations, the generated load scenarios and their corresponding probability are listed in Table 1.

TABLE 1. The load scenarios and the corresponding probabilities.

Load Scenario	π_L	Loading %
$L1$	0.1587	54.7486
$L2$	0.6827	70.0000
$L3$	0.1587	85.2514

B. THE UNCERTAINTY OF THE WIND SPEED

Weibull PDF is employed for modelling the uncertainty of the wind speed as follows [39]:

$$PDF_v(v)=\left(\frac{\beta}{\alpha}\right)\left(\frac{v}{\alpha}\right)^{(\beta-1)} exp\left[-\left(\frac{v}{\alpha}\right)^{\beta}\right] \quad 0 \le v < \infty \tag{21}$$

where β and α represent the shape and the scale parameters of the Weibull PDF, the values of α and β are adopted to be 10.0434 and 2.5034, respectively, as given in [38]. The output power of the wind turbine $P_{wg}(v)$ as in terms of the wind speed and rated power is defined as follows [40]:

$$P_{wg}(v) = \begin{cases} 0 & for\ v < v_i \& v > v_o \\ P_{wr}\left(\dfrac{v - v_{\omega i}}{v_{\omega r} - v_{\omega i}}\right) & for\ (v_i \le v \le v_r) \\ P_{wr} & for\ (v_r < v \le v_o) \end{cases} \tag{22}$$

where P_{wr} is the wind turbine rated power; $v_{\omega i}$ is the cut-in speed, $v_{\omega r}$ is the rated speed, and $v_{\omega o}$ is the cut-out speed of the wind turbine. The portability of wind speed for each scenario is obtained as follows [38], [41]:

$$\pi_{w,k} = \int_{v_k^{min}}^{v_k^{max}} PDF_v(v)dv \tag{23}$$

$$v_{,k} = \frac{1}{\pi_{L,i}} \int_{v_k^{min}}^{v_k^{max}} v \times PDF_v(v)dv \tag{24}$$

where $\pi_{w,k}$ is the wind speed probability in scenario k; v_k^{min} and v_k^{max} denote the starting and ending points of wind speed's interval at k-th scenario, respectively. Three scenarios for wind speed are generated from the previous equations. The probability of the scenarios and the corresponding wind speed are shown in Table 2.

TABLE 2. Scenarios of the wind speed and the corresponding probabilities.

Wind Scenario	π_w	Wind speed (m/s)
$k1$	0.6281	6.5493
$k2$	0.3066	12.0574
$k3$	0.0652	16.8690

C. MODELING THE UNCERTAINTY OF THE SOLAR IRRADIANCE

Beta PDF is employed for modelling the uncertainty of solar irradiance (G), which can be described as follows [42]:

$$PDF_s(G) = \begin{cases} \dfrac{\Gamma(\alpha+\beta)}{\Gamma(\alpha)+\Gamma(\beta)} \times G^{\propto-1} \\ \times (1-G)^{\beta-1} & If\ 0 \le G \\ 0 & otherwise \end{cases} \le 1, 0 \le \alpha, \beta \tag{25}$$

where Γ denotes the gamma function; α and β represent the parameters of the beta PDF which is calculated using (26) and (27)

$$\beta = (1-\mu_s) \times \left(\frac{\mu_s \times (1+\mu_s)}{{\sigma_s}^2}\right) - 1 \tag{26}$$

$$\alpha = \left(\frac{\mu_s \times \beta}{(1-\mu_s)}\right) - 1 \tag{27}$$

where, σ_s the standard deviation is the while μ_s is the mean value of the solar irradiance. The selected values of α and β are 6.38 and 3.43, respectively, as given in [43]. The output power of the PV system depends upon the solar irradiance, and it can be assigned using (28) as follows [44], [45].

$$P_s(G) = \begin{cases} P_{sr}\left(\dfrac{G^2}{G_{std} \times X_c}\right) & for\ 0 < G \le X_c \\ P_{sr}\left(\dfrac{G}{G_{std}}\right) & for\ G \ge X_c \end{cases} \tag{28}$$

where P_{sr} denotes the rated power of the solar PV units. G_{std} represents the standard solar irradiance, which is set as 1000 W/m^2. X_c represents a certain irradiance point, which is set as 120 W/m^2 [28].

The portability and the corresponding of solar irradiance for each scenario can be calculated as follows [41]:

$$\pi_{G,m} = \int_{G_m^{min}}^{G_m^{max}} PDF_s(G)dG \tag{29}$$

$$G_{,m} = \frac{1}{\pi_{s,m}} \int_{G_m^{min}}^{G_m^{max}} G \times PDF_s(v)dG \tag{30}$$

where $\pi_{s,m}$ represents the probability of the solar irradiance of m-th scenario. G_m^{min} and G_m^{max} denote the lower and upper points of solar irradiances of m-th scenario. In this paper, three scenarios of the solar irradiance are generated where the probabilities of these scenarios and the corresponding irradiance are depicted in Table 3.

TABLE 3. The solar irradiance scenarios with the corresponding probabilities.

Irradiance Scenario	π_G	Solar irradiance W/m^2
$m1$	0.1605	416.0627
$m2$	0.4412	609.1166
$m3$	0.3983	790.4621

A scenario-based method is employed to obtain a set of scenarios from the above scenarios by combining the load,

wind, and solar irradiance scenarios, their probabilities are obtained as follows:

$$\pi_S = \pi_{L,i} \times \pi_{w,k} \times \pi_{G,m} \tag{31}$$

IV. OVERVIEW OF LAPO

LAPO technique mimics the mechanism of the lightning phenomena. lightning occurrence is based on four steps describe the main this phenomenon, including breakdown of the air, the descending leader movement, the ascending leader motion, and the strike point.

A. LAPO ALGORITHM

1) AIR BREAKDOWN

The charges formation in the cloud is shown in Figure 1, it is obvious that large amount of negative charges are existed at the bottom with a small quantity of the positive charges while a huge quantities of positive charges are located at the top of the cloud. The amount of charges increase which leads to the breakdown inside the cloud and increasing the voltage of the cloud edges [32], [33].

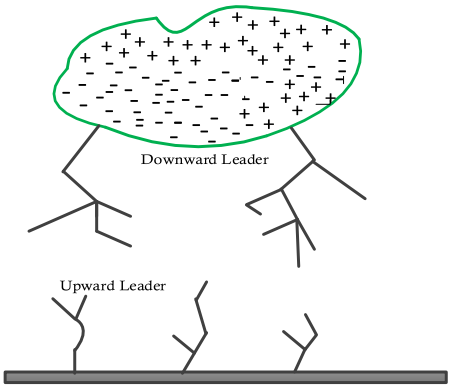

FIGURE 1. Formation of leader and charges the clouds.

2) MOTION OF THE DOWNWARD LEADER TO THE GROUND

The motion of lightning to the ground is in steps. After each step, the lightning will be stopped, while in the next movement, the lightning goes to earth in one or more directions, which represents the downward leader. To mimic the lightning procedure, consider a half-sphere is existed after finishing each procedure, below the leader slant allied to its middle point and circles of the upcoming step, as shown in Figure 2. The half-sphere includes several potential points which have been followed for the next leap point. The updated points are randomly selected which has a higher value of the electrical field.

3) BRANCH VANISHES

The next point is splinted into several points to form several branches. With occurrence this step is repeated the air breakdown until absence of breakdown. The branches will stop and disappear.

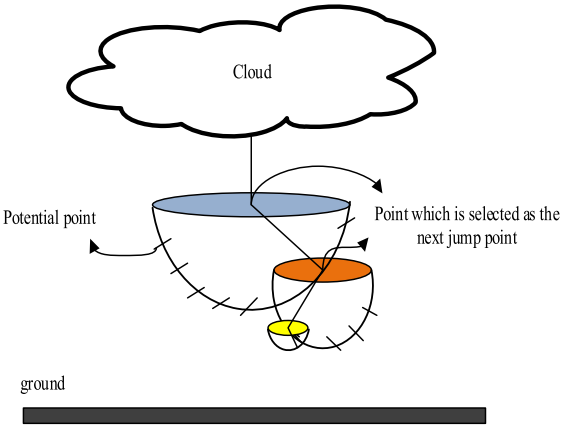

FIGURE 2. Motion of Downward leader to earth.

4) UPWARD LEADER SPREAD

As mentioned before, due to accumulation a huge of negative charge at the bottom of the cloud. Consequently, the positive charges will appear at the ground at the sharp points. Increasing the amount of these charges, the air breakdown will occur, and the upward leader emerged from these sharp points. The upward leaders move to the earth to be combined with the downward leader faster.

5) FINAL JUMP

The final jump point denotes the point that the upward and the downward leaders are combined. This point represents the strike point where the branches are vanished, which leads to neutral charge.

B. MATHEMATICAL REPRESNTATION OF LAPO

The mathematical representation of LAPO are depicted using the listed steps as follows:

Step 1: Initialization

Initial search agents represent the initial test points which denote the starting points of the upward leaders. These points are generated randomly using (32)

$$X_s^i = X_{min}^i + \left(X_{max}^i - X_{min}^i\right) \times rand \tag{32}$$

where X_{min}^i denotes the minimum of the i-th variable while X_{max}^i denotes the maximum limits, respectively. *rand* denotes the random number in the range [0,1]. The fitness functions of the initial points are calculated as follows:

$$F_s^i = obj(X_s^i) \tag{33}$$

Step 2: The next jump determination

The average point (X_{avr}) is assigned and also its corresponding fitness function (F_{avr}).

$$X_{avr} = mean(X_s) \tag{34}$$

$$F_{avr} = obj(X_{avr}) \tag{35}$$

For updating the location of the point (population) anther point randomly j where $i \neq j$ is selected and a comparison

TABLE 4. Simulation results for ORPD problem solution for case 1.

Control variables	Min.	Max.	P_{Loss} minimization		TVD minimization	
			ILAPO	LAPO	ILAPO	LAPO
Generator voltage						
$V1(p.u)$	0.9	1.1	1.1000	1.1000	0.9942	1.0286
$V2(p.u)$	0.9	1.1	1.0944	1.0953	0.9563	0.9702
$V5(p.u)$	0.9	1.1	1.0944	1.0756	1.0689	1.0683
$V8(p.u)$	0.9	1.1	1.0767	1.0789	0.9919	0.9983
$V11(p.u)$	0.9	1.1	1.1000	1.0970	1.0650	1.0134
$V13(p.u)$	0.9	1.1	1.1000	1.0999	1.0436	1.0027
Transformer tap ratio						
T11	0.9	1.1	1.0300	0.9500	1.0900	1.0100
T12	0.9	1.1	0.9000	1.0500	0.9400	0.9700
T15	0.9	1.1	0.9800	1	1.0400	0.9700
T36	0.9	1.1	0.9600	0.9800	0.9800	0.9700
Capacitor banks						
$Q10(p.u)$	0	5	4.9900	4.9800	0.0200	0
$Q12(p.u)$	0	5	5	2.3900	3.9900	2.0400
$Q15(p.u)$	0	5	5	4.7600	4.5000	4.9900
$Q17(p.u)$	0	5	5	4.8700	1.0800	0.3700
$Q20(p.u)$	0	5	3.8000	5	4.6700	4.6400
$Q21(p.u)$	0	5	5	4.8200	0.0200	0.0100
$Q23(p.u)$	0	5	3.3500	3.9000	4.9800	3.8800
$Q24(p.u)$	0	5	5	4.9700	5	4.0100
$Q29(p.u)$	0	5	1.4400	2.2000	4.7900	2.5300
P_{Loss} (MW)			4.5217	4.5428	6.2794	5.6154
TVD $(p.u)$			2.0529	1.8387	**0.0876**	0.0945
$L_{\max}$ (p.u)			0.1152	0.1178	0.1330	0.1343

between the value of the point j and the averaged value as follows:

$$\text{When } f\left(X_{ts}^{j}\right) > f\left(X_{avr}\right)$$
$$X_{s\_new}^{i} = X_{s}^{i} + rand \times \left(X_{avr} + rand \times X_{s}^{j}\right) \quad (36)$$
$$\text{When } f\left(X_{ts}^{j}\right) < f\left(X_{avr}\right)$$
$$X_{s\_new}^{i} = X_{ts}^{i} - rand \times \left(X_{avr} + rand \times X_{ts}^{j}\right) \quad (37)$$

Step 3: Branch vanishes

Branch disappears or vanishes; it can be accomplished by mean acceptance of the new point. The updated obtained point is accepted if it's objective function is better than the original point as follows:

$$X_{s}^{i} = X_{s\_new}^{i} \quad IF\ F_{s\_new}^{i} < F_{s}^{i} \quad (38)$$
$$X_{s\_new}^{i} = X_{s}^{i} \quad otherwise \quad (39)$$

These steps will be applied for all points, and all test points are taken as downward leaders and moved down.

Step 4: Upward leader motion

In this step, all points are considered upward leaders and go upward. The orientation of the upward leaders follows the motion of the downward leaders, which is controlled by an exponential operator through the channel, which can be modeled using (40) as:

$$X_{s\_new}^{i} = X_{s\_new}^{i} + rand \times H \times (X_{best} - X_{worst}) \quad (40)$$

where:

$$H = 1 - (\frac{t}{t_{max}}) \times exp(-\frac{t}{t_{max}}) \quad (41)$$

where; t_{max} and t denote the maximum and the current numbers of iteration the iteration number, respectively; X_{best} is the best solution; X_{worst} represents the worst solution.

Step 5: Final jump

This step represents the final step of the lightning when it occurs when the down leader and up leader are combined at a specific point called the striking point.

V. OVERVIEW OF ILAPO

LAPO is an effective algorithm to solve several optimization problems. However, it is like several meta- algorithms. It may be prone to local optima and stagnation in some cases. The proposed ILAPO is based on emphases the searching ability of the traditional LAPO by enhancing its exploration and exploitation phases. The exploration phase at the first iterative process is adapted by updating the placement of the test points randomly using the Levy Flight as follows [46], [47]:

$$X_{s\_new}^{i} = X_{s}^{i} + \propto \oplus Levy\,(\beta) \quad (42)$$

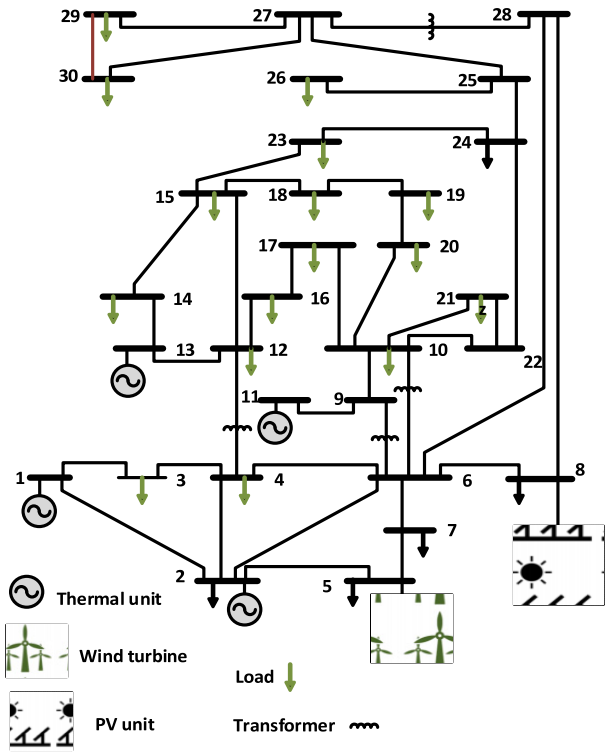

FIGURE 3. The modified IEEE 30-bus system.

where $\propto$ represents a step size parameter which can be obtained as follows:

$$\propto \oplus Levy(\beta) \sim 0.01 \frac{u}{|v|^{1/\beta}} \left(X_s^i - X_{best}\right) \tag{43}$$

where u and v can be found from (44) and (45) as follows:

$$u \sim N\left(0, \phi_u^2\right), \quad v \sim N\left(0, \phi_v^2\right) \tag{44}$$

$$\phi_u = \left[\frac{\Gamma(1+\beta) \times sin(\pi \times \beta/2)}{\Gamma[(1+\beta)/2] \times \beta}\right]^{1/\beta}, \quad \phi_v = 1 \tag{45}$$

where Γ denotes the standard gamma function. In the final iterative process, the exploitation phase is improved by updating the points around the best solution in a spiral pass using a logarithmic spiral function as follows:

$$X_{s\_new}^i = \left|X_{best} - X_s^i\right| e^{bt} \cos(2\pi t) + X_{best} \tag{46}$$

where b denotes a constant to define the logarithmic spiral shape.

VI. SIMULATION RESULTS

The proposed algorithm in this section is applied to addresses the ORPD, and it is tested on the IEEE 30-bus system. The program code for solving the ORPD was written by MATLAB software, and it has been performed on a Core I5 PC with 4GB RAM. The IEEE 30-bus system has six thermal generation units at bus#1, bus #2, bus #5, bus #8, bus #11, and bus #13. The system branches and bus data are captured in [20]. The control variables limits are tabulated in Table 4, and the step size of transformer taps, and the injected capacitor reactive power are 0.01 p.u. The ORPD is solved with and without taken into consideration the stochastics nature or the uncertainties of the RERs and load demand where the IEEE 30-bus is modified by adding wind turbines at bus 5 and PV units at bus 8 as depicted in Figure 3. The selected search agent and maximum iteration numbers for all

TABLE 5. Comparison of P_{Loss} minimization by application different optimization algorithm.

Algorithm	Worst	Mean	Best
ILAPO	4.559761	4.527079	**4.521717**
LAPO	4.783423	4.631454	4.542848
JA [12]	NR	NR	4.625
ALO [4]	NR	NR	4.5900
HSA[48]	4.9653	4.924	4.9059
PSO [48]	5.0576	4.972	4.9239
STGA [48]	5.1651	5.0378	4.9408
TLBO [17]	4.57480	4.56950	4.5629
QOTLBO [17]	4.56170	4.56010	4.5594
DE [8]	NR	NR	4.5550
SGA [49]	NR	NR	4.5692
FA [23]	4.59	4.578	4.5691
HPSO–TS [50]	NR	NR	4.5213
TS [50]	NR	NR	4.9203
PSO [50]	NR	NR	4.6862
WOA [6]	NR	NR	4.5943
PSO-TVAC[6]	NR	NR	4.6469
IDE [11]	NR	NR	4.5521
BBO [16]	NR	NR	4.5511
CLPSO[19]	NR	NR	4.6282
PSO[19]	NR	NR	4.5615
GSA [21]	NR	NR	5.00954
PSO [21]	NR	NR	4.91578
GSA-CSS [21]	NR	NR	4.79301
IGSA-CSS [21]	NR	NR	4.76601

TABLE 6. Comparison of *TVD* minimization by application different optimization algorithms.

Algorithm	Worst	Mean	Best
ILAPO	0.1542636	0.1106569	0.08756657
LAPO	0.112352	0.1546573	0.09453693
QOTLBO [17]	0.0907	0.0872	0.0856
TLBO [17]	0.0988	0.0934	0.0913
PSO-TVIW [22]	0.5791	0.1597	0.1038
PSO-TVA [22]	0.5796	0.2376	0.2064
SPSO-TVAC [22]	0.1833	0.1558	0.1354
PSO-CF [22]	0.4041	0.1557	0.1287
PG-PSO [22]	0.2593	0.1440	0.1202
SWT-PSO [22]	0.2296	0.1814	0.1614
IPG-PSO [22]	0.2518	0.1078	0.0892
DE [8]	NR	NR	0.0911
ISSO [7]	0.14938	0.11603	0.08847
SSO [7]	0.42681	0.2863	0.19304
HSSSA [7]	0.576439	0.308337	0.174701
MSSA [7]	1.860037	0.690254	0.230087
SSA [7]	0.941759	0.374529	0.188411
CSA [7]	0.2076	0.16432	0.12692
IALO [5]	NR	0.1012	0.0881
ALO [5]	NR	0.1575	0.1192
GSA [21]	NR	NR	0.17241
PSO [21]	NR	NR	0.10462
GSA-CSS [21]	NR	NR	0.12394
IGSA-CSS [21]	NR	NR	0.08968

TABLE 7. The percentage of loads, solar irradiances, the wind speeds, and their corresponding probabilities.

Scenario	Loading %	Solar irradiance (W/m^2)	Wind speed (m/s)	π_L	π_G	π_w	π_S
$S1$	54.7486	416.0627	6.5493	0.1587	0.1605	0.6281	0.0160
$S2$	54.7486	416.0627	12.0574	0.1587	0.1605	0.3066	0.0078
$S3$	54.7486	416.0627	16.8690	0.1587	0.1605	0.0652	0.0017
$S4$	54.7486	609.1166	6.5493	0.1587	0.4412	0.6281	0.0440
$S5$	54.7486	609.1166	12.0574	0.1587	0.4412	0.3066	0.0215
$S6$	54.7486	609.1166	16.8690	0.1587	0.4412	0.0652	0.0046
$S7$	54.7486	790.4621	6.5493	0.1587	0.3983	0.6281	0.0397
$S8$	54.7486	790.4621	12.0574	0.1587	0.3983	0.3066	0.0194
$S9$	54.7486	790.4621	16.8690	0.1587	0.3983	0.0652	0.0041
$S10$	70.0000	416.0627	6.5493	0.6827	0.1605	0.6281	0.0688
$S11$	70.0000	416.0627	12.0574	0.6827	0.1605	0.3066	0.0336
$S12$	70.0000	416.0627	16.8690	0.6827	0.1605	0.0652	0.0071
$S13$	70.0000	609.1166	6.5493	0.6827	0.4412	0.6281	0.1892
$S14$	70.0000	609.1166	12.0574	0.6827	0.4412	0.3066	0.0924
$S15$	70.0000	609.1166	16.8690	0.6827	0.4412	0.0652	0.0196
$S16$	70.0000	790.4621	6.5493	0.6827	0.3983	0.6281	0.1708
$S17$	70.0000	790.4621	12.0574	0.6827	0.3983	0.3066	0.0834
$S18$	70.0000	790.4621	16.8690	0.6827	0.3983	0.0652	0.0177
$S19$	85.2514	416.0627	6.5493	0.1587	0.1605	0.6281	0.0160
$S20$	85.2514	416.0627	12.0574	0.1587	0.1605	0.3066	0.0078
$S21$	85.2514	416.0627	16.8690	0.1587	0.1605	0.0652	0.0017
$S22$	85.2514	609.1166	6.5493	0.1587	0.4412	0.6281	0.0440
$S23$	85.2514	609.1166	12.0574	0.1587	0.4412	0.3066	0.0215
$S24$	85.2514	609.1166	16.8690	0.1587	0.4412	0.0652	0.0046
$S25$	85.2514	790.4621	6.5493	0.1587	0.3983	0.6281	0.0397
$S26$	85.2514	790.4621	12.0574	0.1587	0.3983	0.3066	0.0194
$S27$	85.2514	790.4621	16.8690	0.1587	0.3983	0.0652	0.0041

studied cases are 30 and 100, respectively, while the number of trial runs is 30. The case studies are listed as follows:

A. CASE 1: SOLVING THE ORPD WITHOUT RERs

The aim of addressing the ORPD solution here is to diminish the power losses (P_{Loss}) and summation voltage deviations (TVD) without considering RERs. The simulation results, including the optimized variables by ILAPO and LAPO, are tabulated in Table 5. The power losses by applying ILAPO and LAPO are 4.5217 MW and 4.5428 MW. Table 6 shows a comparison of the obtained results for power losses minimization by several optimization algorithms. Judging from Table 6, the minimum power losses are achieved by applying the proposed algorithm compared with the traditional LAPO and the other reported techniques. The obtained TVD by using ILAPO and LAPO are 0.0876 p.u and 0.0903 p.u, respectively. Table 6 shows a comparison of the captured results of the TVD by other algorithms. referring to Table 6; the achieved TVD by using the proposed algorithm is less than the traditional LAPO and the other listed techniques. Figures 4 and 5 show the trends of the P_{Loss} and TVD by application of ILAPO and LAPO. According to these figures, the proposed algorithm has stable performance characteristics without oscillation.

B. CASE 2: SOLVING THE ORPD CONSIDERING THE UNCERTAINTIES OF LOAD DEMAND AND RERs

The aim of the ORPD solution here is reducing the expected power losses under the uncertainties of load demand and

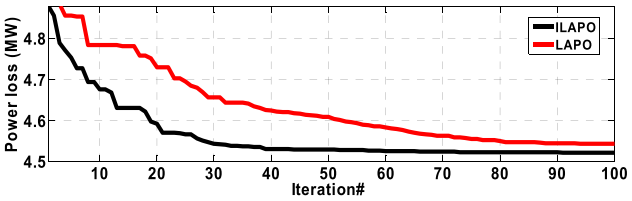

FIGURE 4. The trends of the P_{Loss} with LAPO and ILAPO technique.

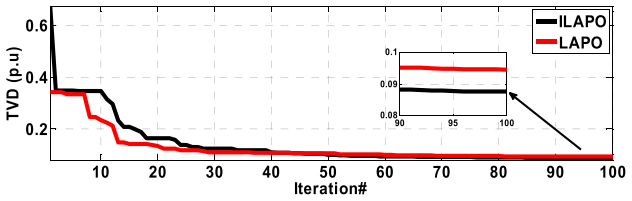

FIGURE 5. The trends of the TVD with LAPO and ILAPO technique.

RERs, which based on the uncertainties of wind speed (v) and solar irradiance (G). In the modified IEEE 30-bus system, a wind farm and solar PV system are incorporated in bus 5 and bus 8, respectively. The wind farm contains 25 turbines, and the turbine rated power is 3 MW, while its $v_{\omega r}$ $v_{\omega o}$ and $v_{\omega i}$ are 16 m/s, 25m/s, and 3m/s, respectively. The rated power of the PV system is 50 MW and G_{std} is 1000 W/ m^2 [31].

In this case, a combination of the probabilities of the solar irradiance, the load, and the wind speed using the scenario-based method are performed. In sequent 27 scenarios are produced. The generated scenarios and the equivalent

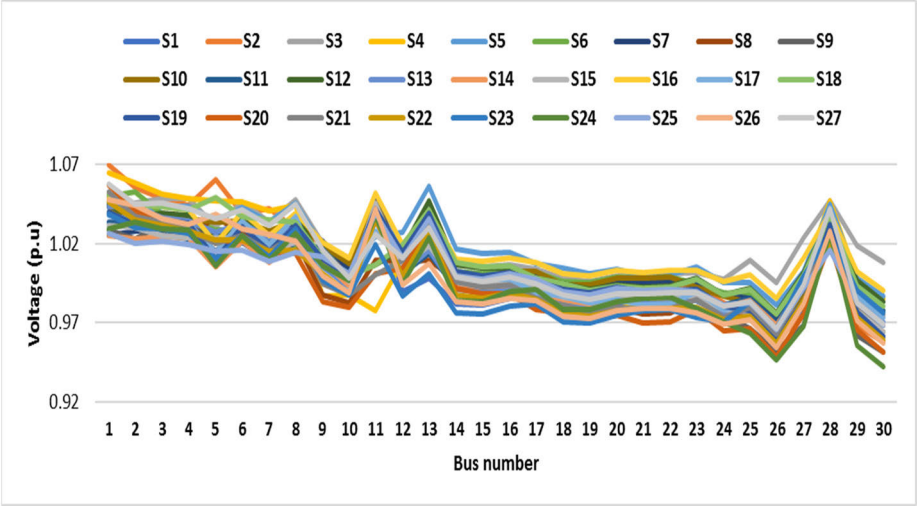

FIGURE 6. The voltage profile of the IEE 30-bus system for each scenario.

TABLE 8. The generated power of the RERs, the power losses and the expected power losses for all scenarios.

Scenario	π_S	$P_s(MW)$	$P_{wg}(MW)$	LAPO		ILAPO	
				$P_{Loss}(MW)$	$EPL(MW)$	$P_{Loss}(MW)$	$EPLMW)$
$S1$	0.0160	20.8031	20.4767	1.2896	0.0206	1.2122	0.0194
$S2$	0.0078	20.8031	52.2542	1.0770	0.0084	1.4561	0.0114
$S3$	0.0017	20.8031	75.0000	1.6519	0.0028	1.4913	0.0025
$S4$	0.0440	30.4558	20.4767	1.1799	0.0519	1.2377	0.0545
$S5$	0.0215	30.4558	52.2542	1.1788	0.0253	1.1378	0.0245
$S6$	0.0046	30.4558	75.0000	1.4633	0.0067	1.7882	0.0082
$S7$	0.0397	39.5231	20.4767	1.2408	0.0493	1.1260	0.0447
$S8$	0.0194	39.5231	52.2542	1.1916	0.0231	1.5277	0.0296
$S9$	0.0041	39.5231	75.0000	2.8501	0.0117	1.9125	0.0078
$S10$	0.0688	20.8031	20.4767	2.5322	0.1742	2.4750	0.1703
$S11$	0.0336	20.8031	52.2542	1.5647	0.0526	1.4488	0.0487
$S12$	0.0071	20.8031	75.0000	1.3211	0.0094	1.4434	0.0102
$S13$	0.1892	30.4558	20.4767	2.1123	0.3996	2.0968	0.3967
$S14$	0.0924	30.4558	52.2542	1.2841	0.1186	1.3358	0.1234
$S15$	0.0196	30.4558	75.0000	1.2957	0.0254	1.2427	0.0244
$S16$	0.1708	39.5231	20.4767	2.0376	0.3480	1.9184	0.3277
$S17$	0.0834	39.5231	52.2542	1.1824	0.0986	1.3529	0.1128
$S18$	0.0177	39.5231	75.0000	1.2385	0.0219	1.3422	0.0238
$S19$	0.0160	20.8031	20.4767	4.7982	0.0768	4.5932	0.0735
$S20$	0.0078	20.8031	52.2542	3.0551	0.0238	2.9816	0.0233
$S21$	0.0017	20.8031	75.0000	2.2091	0.0038	2.2826	0.0039
$S22$	0.0440	30.4558	20.4767	4.2850	0.1885	4.1014	0.1805
$S23$	0.0215	30.4558	52.2542	2.6299	0.0565	2.5145	0.0541
$S24$	0.0046	30.4558	75.0000	2.0157	0.0093	2.0556	0.0095
$S25$	0.0397	39.5231	20.4767	3.7424	0.1486	3.8404	0.1525
$S26$	0.0194	39.5231	52.2542	2.4689	0.0479	2.2560	0.0438
$S27$	0.0041	39.5231	75.0000	1.9872	0.0081	1.7830	0.0073
$Total\_EPL(MW)$					2.0116		1.9887

probabilities are given in Table 7. The main target of solving the ORPD with the uncertainties of the system, to minimize the expected power losses, which can be determined as follows:

$$Total\_EPL = \sum_{n=1}^{27} EPL_n = \sum_{n=1}^{27} \pi_{S,n} \times P_{Loss,n} \quad (47)$$

where $Total\_EPL$ denotes the total expected power losses; EPL_n denotes the expected power losses of i-th scenario; $\pi_{S,i}$ denotes the probability of n-th scenario. Table 8 shows the output powers of the solar and wind systems, the power losses and the EPL for each scenario. The $Total\_EPL$ without inclusion RERs is 5.0003 MW while the $Total\_EPL$ that gained by LAPO and ILAPO 2.0116 MW and 1.9887 MW, respectively. Figure 5 illustrates the voltage profile of the system for all scenarios. The voltage profiles for all scenarios are within the allowable limits, which is [0.9- 1.10] p.u.

VII. CONCLUSION

This paper has presented an efficient Improved Lightning Attachment Procedure Optimization Algorithm to address the ORPD problem. Minimizing the system active losses and the voltage deviations under deterministic and probabilistic conditions have been considered. Two improvements have been applied to the traditional LAPO technique, including Levy Flight distribution for enhancing the exploration of the algorithm and a logarithmic spiral movement of the test points around the optimal solution for enhancing the exploitation of the algorithm. The ORPD problem has been addressed under three uncertain parameters, load demand, the wind speed of the wind turbines, and the solar irradiance of the PV unit, which have been represented by the normal PDF, Weibull PDF, and Beta PDF respectively. A set of scenarios is obtained by a combination of these uncertainties for minimizing the expected power losses. The proposed ILAPO was tested on the IEEE 30-bus system. The obtained results verified that the minimum power losses and voltage deviations obtained by applying the proposed improved technique compared with LAPO and the other reported optimization techniques. Furthermore, the expected power losses at uncertainties of the system is minimized by 60.23 % compared with the base case.

ACKNOWLEDGMENT

The authors gratefully acknowledge the contribution of the NSFC, China-ASRT, Egypt, Joint Research Fund, under Project 51861145406 for providing partial research funding to the work reported in this research.

REFERENCES

[1] M. S. Saddique, A. R. Bhatti, S. S. Haroon, M. K. Sattar, S. Amin, I. A. Sajjad, S. S. ul Haq, A. B. Awan, and N. Rasheed, "Solution to optimal reactive power dispatch in transmission system using meta-heuristic techniques—Status and technological review," *Electr. Power Syst. Res.*, vol. 178, Jan. 2020, Art. no. 106031.

[2] A. M. Shaheen, R. A. El-Sehiemy, and S. M. Farrag, "Integrated strategies of backtracking search optimizer for solving reactive power dispatch problem," *IEEE Syst. J.*, vol. 12, no. 1, pp. 424–433, Mar. 2018.

[3] B. Zhao, C. X. Guo, and Y. J. Cao, "A multiagent-based particle swarm optimization approach for optimal reactive power dispatch," *IEEE Trans. Power Syst.*, vol. 20, no. 2, pp. 1070–1078, May 2005.

[4] S. Mouassa, T. Bouktir, and A. Salhi, "Ant lion optimizer for solving optimal reactive power dispatch problem in power systems," *Eng. Sci. Technol., Int. J.*, vol. 20, no. 3, pp. 885–895, Jun. 2017.

[5] Z. Li, Y. Cao, L. V. Dai, X. Yang, and T. T. Nguyen, "Finding solutions for optimal reactive power dispatch problem by a novel improved antlion optimization algorithm," *Energies*, vol. 12, no. 15, p. 2968, Aug. 2019.

[6] K. B. O. Medani, S. Sayah, and A. Bekrar, "Whale optimization algorithm based optimal reactive power dispatch: A case study of the Algerian power system," *Electr. Power Syst. Res.*, vol. 163, pp. 696–705, Oct. 2018.

[7] T. T. Nguyen and D. N. Vo, "Improved social spider optimization algorithm for optimal reactive power dispatch problem with different objectives," *Neural Comput. Appl.*, vol. 32, pp. 5919–5950, Feb. 2019.

[8] A. A. A. El Ela, M. A. Abido, and S. R. Spea, "Differential evolution algorithm for optimal reactive power dispatch," *Electr. Power Syst. Res.*, vol. 81, no. 2, pp. 458–464, Feb. 2011.

[9] S. Abdel-Fatah, M. Ebeed, S. Kamel, and L. Nasrat, "Moth swarm algorithm for reactive power dispatch considering stochastic nature of renewable energy generation and load," in *Proc. 21st Int. Middle East Power Syst. Conf. (MEPCON)*, Dec. 2019, pp. 594–599.

[10] Q. H. Wu and J. T. Ma, "Power system optimal reactive power dispatch using evolutionary programming," *IEEE Trans. Power Syst.*, vol. 10, no. 3, pp. 1243–1249, 1995.

[11] D. Prasad, A. Banerjee, and R. P. Singh, "Optimal reactive power dispatch using modified differential evolution algorithm," in *Advances in Computer, Communication and Control*. Singapore: Springer, 2019, pp. 275–283.

[12] S. Mandal, K. K. Mandal, and S. Kumar, "A new optimization technique for optimal reactive power scheduling using Jaya algorithm," in *Proc. Innov. Power Adv. Comput. Technol. (i-PACT)*, Apr. 2017, pp. 1–5.

[13] S. Abdel-Fatah, M. Ebeed, and S. Kamel, "Optimal reactive power dispatch using modified sine cosine algorithm," in *Proc. Int. Conf. Innov. Trends Comput. Eng. (ITCE)*, Feb. 2019, pp. 510–514.

[14] S. Abdel-Fatah, M. Ebeed, S. Kamel, and J. Yu, "Reactive power dispatch solution with optimal installation of renewable energy resources considering uncertainties," in *Proc. IEEE Conf. Power Electron. Renew. Energy (CPERE)*, Oct. 2019, pp. 118–123.

[15] S. Duman, Y. Sönmez, U. Güvenç, and N. Yörükeren, "Optimal reactive power dispatch using a gravitational search algorithm," *IET Gener., Transmiss. Distrib.*, vol. 6, no. 6, pp. 563–576, Jun. 2012.

[16] A. Bhattacharya and P. K. Chattopadhyay, "Solution of optimal reactive power flow using biogeography-based optimization," *Int. J. Electr. Electron. Eng.*, vol. 4, no. 8, pp. 568–576, 2010.

[17] B. Mandal and P. K. Roy, "Optimal reactive power dispatch using quasi-oppositional teaching learning based optimization," *Int. J. Electr. Power Energy Syst.*, vol. 53, pp. 123–134, Dec. 2013.

[18] S. Kamel, S. Abdel-Fatah, M. Ebeed, J. Yu, K. Xie, and C. Zhao, "Solving optimal reactive power dispatch problem considering load uncertainty," in *Proc. IEEE Innov. Smart Grid Technol. - Asia (ISGT Asia)*, May 2019, pp. 1335–1340.

[19] K. Mahadevan and P. S. Kannan, "Comprehensive learning particle swarm optimization for reactive power dispatch," *Appl. Soft Comput.*, vol. 10, no. 2, pp. 641–652, Mar. 2010.

[20] S. Dutta, P. K. Roy, and D. Nandi, "Optimal location of STATCOM using chemical reaction optimization for reactive power dispatch problem," *Ain Shams Eng. J.*, vol. 7, no. 1, pp. 233–247, Mar. 2016.

[21] G. Chen, L. Liu, Z. Zhang, and S. Huang, "Optimal reactive power dispatch by improved GSA-based algorithm with the novel strategies to handle constraints," *Appl. Soft Comput.*, vol. 50, pp. 58–70, Jan. 2017.

[22] J. Polprasert, W. Ongsakul, and V. N. Dieu, "Optimal reactive power dispatch using improved pseudo-gradient search particle swarm optimization," *Electric Power Compon. Syst.*, vol. 44, no. 5, pp. 518–532, Mar. 2016.

[23] A. Rajan and T. Malakar, "Optimal reactive power dispatch using hybrid Nelder–Mead simplex based firefly algorithm," *Int. J. Electr. Power Energy Syst.*, vol. 66, pp. 9–24, Mar. 2015.

[24] N. Habib Khan, Y. Wang, D. Tian, M. A. Z. Raja, R. Jamal, and Y. Muhammad, "Design of fractional particle swarm optimization gravitational search algorithm for optimal reactive power dispatch problems," *IEEE Access*, vol. 8, pp. 146785–146806, 2020.

[25] M. A. M. Shaheen, H. M. Hasanien, and A. Alkuhayli, "A novel hybrid GWO-PSO optimization technique for optimal reactive power dispatch problem solution," *Ain Shams Eng. J.*, Aug. 2020, doi: 10.1016/j.asej.2020.07.011.

[26] S. Mahapatra, S. Raj, and S. M. Krishna, "Optimal TCSC location for reactive power optimization using oppositional salp swarm algorithm," in *Innovation in Electrical Power Engineering, Communication, and Computing Technology*. Singapore: Springer, 2020, pp. 413–424.

[27] M. Vishnu and S. K. T. K., "An improved solution for reactive power dispatch problem using diversity-enhanced particle swarm optimization," *Energies*, vol. 13, no. 11, p. 2862, Jun. 2020.

[28] P. P. Biswas, P. N. Suganthan, R. Mallipeddi, and G. A. J. Amaratunga, "Optimal reactive power dispatch with uncertainties in load demand and renewable energy sources adopting scenario-based approach," *Appl. Soft Comput.*, vol. 75, pp. 616–632, Feb. 2019.

[29] M. Naidji and M. Boudour, "Stochastic multi-objective optimal reactive power dispatch considering load and renewable energy sources uncertainties: A case study of the Adrar isolated power system," *Int. Trans. Electr. Energy Syst.*, vol. 30, no. 6, p. e12374, 2020.

[30] S. M. Mohseni-Bonab, A. Rabiee, and B. Mohammadi-Ivatloo, "Voltage stability constrained multi-objective optimal reactive power dispatch under load and wind power uncertainties: A stochastic approach," *Renew. Energy*, vol. 85, pp. 598–609, Jan. 2016.

[31] S. M. Mohseni-Bonab, A. Rabiee, B. Mohammadi-Ivatloo, S. Jalilzadeh, and S. Nojavan, "A two-point estimate method for uncertainty modeling in multi-objective optimal reactive power dispatch problem," *Int. J. Electr. Power Energy Syst.*, vol. 75, pp. 194–204, Feb. 2016.
[32] A. F. Nematollahi, A. Rahiminejad, and B. Vahidi, "A novel physical based meta-heuristic optimization method known as lightning attachment procedure optimization," *Appl. Soft Comput.*, vol. 59, pp. 596–621, Oct. 2017.
[33] A. F. Nematollahi, A. Rahiminejad, and B. Vahidi, "A novel multi-objective optimization algorithm based on lightning attachment procedure optimization algorithm," *Appl. Soft Comput.*, vol. 75, pp. 404–427, Feb. 2019.
[34] M. A. Taher, S. Kamel, F. Jurado, and M. Ebeed, "Optimal power flow solution incorporating a simplified UPFC model using lightning attachment procedure optimization," *Int. Trans. Electr. Energy Syst.*, vol. 30, no. 1, Jan. 2020.
[35] H. Youssef, S. Kamel, and M. Ebeed, "Optimal power flow considering loading margin stability using lightning attachment optimization technique," in *Proc. 20th Int. Middle East Power Syst. Conf. (MEPCON)*, Dec. 2018, pp. 1053–1058.
[36] P. Hashemian, A. F. Nematollahi, and B. Vahidi, "A novel approach for optimal DG allocation in distribution network for minimizing voltage sag," *Adv. Energy Res.*, vol. 6, no. 1, pp. 55–73, 2019.
[37] W. Liu, S. Yang, Z. Ye, Q. Huang, and Y. Huang, "An image segmentation method based on two-dimensional entropy and chaotic lightning attachment procedure optimization algorithm," *Int. J. Pattern Recognit. Artif. Intell.*, Mar. 2020, Art. no. 2054030.
[38] S. M. Mohseni-Bonab and A. Rabiee, "Optimal reactive power dispatch: A review, and a new stochastic voltage stability constrained multi-objective model at the presence of uncertain wind power generation," *IET Gener., Transmiss. Distrib.*, vol. 11, no. 4, pp. 815–829, Mar. 2017.
[39] S. Wen, H. Lan, Q. Fu, D. C. Yu, and L. Zhang, "Economic allocation for energy storage system considering wind power distribution," *IEEE Trans. Power Syst.*, vol. 30, no. 2, pp. 644–652, Mar. 2015.
[40] J. Hetzer, D. C. Yu, and K. Bhattarai, "An economic dispatch model incorporating wind power," *IEEE Trans. Energy Convers.*, vol. 23, no. 2, pp. 603–611, Jun. 2008.
[41] Y. M. Atwa, E. F. El-Saadany, M. M. A. Salama, and R. Seethapathy, "Optimal renewable resources mix for distribution system energy loss minimization," *IEEE Trans. Power Syst.*, vol. 25, no. 1, pp. 360–370, Feb. 2010.
[42] Z. M. Salameh, B. S. Borowy, and A. R. A. Amin, "Photovoltaic module-site matching based on the capacity factors," *IEEE Trans. Energy Convers.*, vol. 10, no. 2, pp. 326–332, Jun. 1995.
[43] A. R. Jordehi, "How to deal with uncertainties in electric power systems? A review," *Renew. Sustain. Energy Rev.*, vol. 96, pp. 145–155, Nov. 2018.
[44] R.-H. Liang and J.-H. Liao, "A fuzzy-optimization approach for generation scheduling with wind and solar energy systems," *IEEE Trans. Power Syst.*, vol. 22, no. 4, pp. 1665–1674, Nov. 2007.
[45] S. Surender Reddy, P. R. Bijwe, and A. R. Abhyankar, "Real-time economic dispatch considering renewable power generation variability and uncertainty over scheduling period," *IEEE Syst. J.*, vol. 9, no. 4, pp. 1440–1451, Dec. 2015.
[46] G. M. Viswanathan, V. Afanasyev, S. V. Buldyrev, E. J. Murphy, P. A. Prince, and H. E. Stanley, "Lévy flight search patterns of wandering albatrosses," *Nature*, vol. 381, no. 6581, pp. 413–415, May 1996.
[47] M. I. Mosaad, M. Osama abed el-Raouf, M. A. Al-Ahmar, and F. A. Banakher, "Maximum power point tracking of PV system based cuckoo search algorithm; review and comparison," *Energy Procedia*, vol. 162, pp. 117–126, Apr. 2019.
[48] A. H. Khazali and M. Kalantar, "Optimal reactive power dispatch based on harmony search algorithm," *Int. J. Electr. Power Energy Syst.*, vol. 33, no. 3, pp. 684–692, Mar. 2011.
[49] W. Villa-Acevedo, J. López-Lezama, and J. Valencia-Velásquez, "A novel constraint handling approach for the optimal reactive power dispatch problem," *Energies*, vol. 11, no. 9, p. 2352, Sep. 2018.
[50] Z. Sahli, A. Hamouda, A. Bekrar, and D. Trentesaux, "Reactive power dispatch optimization with voltage profile improvement using an efficient hybrid algorithm," *Energies*, vol. 11, no. 8, p. 2134, Aug. 2018.

MOHAMED EBEED received the B.S. degree from Aswan University, in 2005, the M.S. degree in electrical engineering from South Valley University, in 2013, and the jointly-supervised Ph.D. degree from the Department of Electrical Engineering, Faculty of Engineering, Aswan University, Egypt, and the University of Jaen, Spain, in 2018. From 2008 to 2009, he was a Lecturer with the Aswan Technical Institute. From 2009 to 2017, he was a Maintenance Engineer with EFACO Company. He is currently an Assistant Professor with the Department of Electrical Engineering, Faculty of Engineering, Sohag University, Egypt.

ABDELFATAH ALI was born in Egypt, in October 1986. He received the B.Sc. and M.Sc. degrees in electrical engineering from Aswan University, Aswan, Egypt, in 2009 and 2013, respectively, and the Ph.D. degree from the Doctoral School of Electrical Engineering, Faculty of Electrical Engineering and Informatics, Budapest University of Technology and Economics, Budapest, Hungary, in 2019. Since 2010, he has been an Assistant Lecturer with the Faculty of Engineering, South Valley University (SVU), Qena, Egypt, where he is currently an Assistant Professor. His research interests include modeling, analysis, control, and optimization of distribution systems with distributed generation and electric vehicles.

MOHAMED I. MOSAAD received the B.Sc. and M.Sc. degrees in electrical engineering from Zagazig University, Zagazig, Egypt, and the Ph.D. degree in electrical engineering from Cairo University, Cairo, Egypt. He is currently an Associate Professor with the Department of Electrical and Electronics Engineering, Yanbu Industrial College, Saudi Arabia. His research interests include power system stability, control, optimization, and renewable energy.

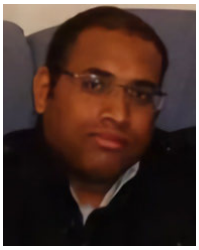

SALAH KAMEL received the International Ph.D. degree from the University of Jaen, Spain, and from Aalborg University, Denmark, in January 2014. He is currently an Associate Professor with the Electrical Engineering Department, Aswan University, Aswan, Egypt. He is also a Leader of the Power Systems Research Group, Advanced Power Systems Research Laboratory (APSR Lab), Aswan. His research interests include power system analysis and optimization, smart grid, and renewable energy systems.